Synthetic Metals 159 (2009) 171–175

Contents lists available at ScienceDirect

Synthetic Metals

journal homepage: www.elsevier.com/locate/synmet

Letter

Perylenetetracarboxylic di-imide-based bottom-contact devices: A study on two kinds of source/drain electrodes, ITO and MoW

ARTICLE INFO

Keywords:
Organic thin-film transistors (OTFTs)
n-Type
Perylene

ABSTRACT

High-performance bottom-contact devices based on an air-stable n-type organic semiconductor N,N-bis(4-trifluoromethoxybenzyl)-perylene-3,4,9,10-tetracarboxylic di-imide, were fabricated, and the effects of crystal packing on indium tin oxide and molybdenum–tungsten alloy were shown in two different electric characteristics. The estimated work function of indium tin oxide and molybdenum–tungsten alloy were 4.7 and 5.0 eV. The calculated lowest unoccupied molecular orbital energy level of the organic material was 3.7 eV. Transistors with indium tin oxide bottom electrodes exhibited a high mobility of 3.37×10^{-2} cm^2 V^{-1} s^{-1}, an on/off current ratio of 6.5×10^5 and threshold voltage of −4.0 V.

1. Introduction

Organic thin-film transistors (OTFTs) are the best candidates for flexible electronic devices. Using organic materials as the semiconductor layer has some advantages, such as low-temperature process, large-area spin coating, inject printing, etc. [1,2]. Pentacene, the hole-transporting material has been widely studied and can be employed in electronic devices [3,4]. For the purpose of making power-efficient complementary metal oxide semiconductor (CMOS) circuits, n-type organic semiconductors must compete with p-type semiconductors [5]. Most electron-transporting (n-type) OTFTs cannot operate in air, because they are sensitive to both oxygen and moisture [6,7]. In recent reports, perylene and naphthalene-based derivatives have demonstrated that high mobilities of ca. 0.1–.7 cm^2 V^{-1} s^{-1} can be used as air-stable n-type materials. In general, OTFTs are fabricated in a top-contact form, in which the source and drain (S/D) electrodes are defined on top of the semiconductor layer through a shadow mask [8]. Yoo et al. reported on high-mobility bottom-contact OTFTs with PDI-8CN$_2$ as n-type organic semiconductors. The device treated with hexamethyldisilazane (HMDS) and 1-octadecanethiol (ODT) showed a mobility of 0.14 cm^2 V^{-1} s^{-1} [9]. The use of self-assembled monolayers (SAMs) which not only caused a lower surface energy of SiO$_2$ (HMDS) but was also employed for ease of charge carrier injection (ODT). However, the disadvantages of SAMs are that they only occur in particular chemical regents, and metal gold, silver or mercury can work with terminal thiol (–SH) groups for example.

We have recently reported N,N-bis(4-trifluoromethoxybenzyl)-1,4,5,8-naphthalene-tetracarboxylic-di-imide (NTCDI-OCF$_3$) as an air-stable n-type organic semiconductor in the fabrication of the bottom-contact device without any surface treatments [10]. The chemical structure which has been modified by "–CF$_3$" seems to reduce the contact resistance at the top-electrode/organic film interface. In order to improve the carrier mobility, the increasing conjugated system of the center-core, naphthalene tetracarboxylic di-anhydride (NTCDA) is replaced by perylene tetracarboxylic di-anhydride (PTCDA) [11]. This is an ideal air-stable, n-type material for in synthesizing a larger conjugated system through two moieties of PTCDA and 4-trifluoromethoxybenzyl amine.

In this letter, we fabricate the bottom-contact device with a new air-stable organic n-type semiconductor, N,N-bis(4-trifluoromethoxybenzyl)-perylene-3,4,9,10-tetracarboxylic di-imide (PTCDI-OCF3). Indium tin oxide (ITO) and molybdenum–tungsten alloy (MoW) are used as two kinds of source/drain (S/D) electrodes in our study. Electron mobility of bottom-contact devices with ITO and MoW as S/D electrodes are 3.37×10^{-2} and 1.11×10^{-2} cm^2 V^{-1} s^{-1}, respectively. All measurements are carried out through a semiconductor analyzer HP 4156A

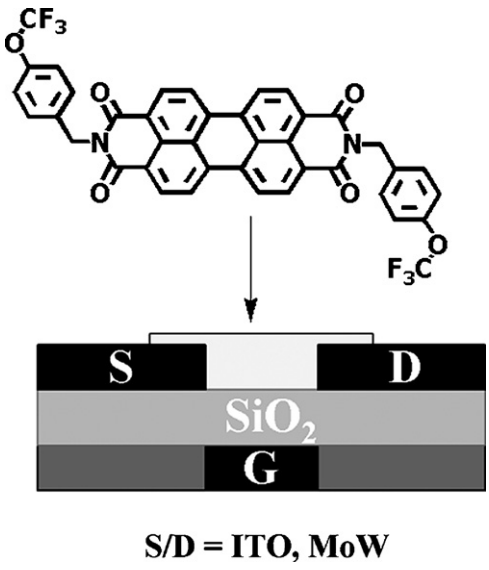

Fig. 1. Schematic diagram of bottom-contact device (channel width/channel length = 500 μm/30 μm) and the chemical structure of PTCDI-OCF$_3$.

0379-6779/$ – see front matter © 2008 Elsevier B.V. All rights reserved.
doi:10.1016/j.synthmet.2008.08.018

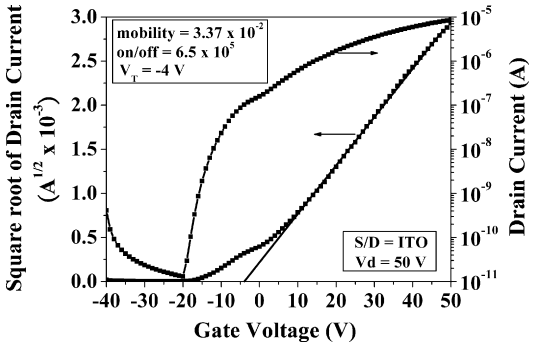

Fig. 2. Transfer characteristics of ITO-based transistors. Inset shows mobility, on/off current ratio (on/off), threshold voltage (V_T), source/drain electrodes (S/D) and drain voltage (V_d).

in air. Fig. 1 shows the chemical structure and the profile of the bottom-contact device with no surface treatments prior to the evaporation of the organic semiconductor.

2. Experimental

For bottom-contact devices, glass was used as substrates and sputtered ITO which served as the gate electrode was patterned on the top of the glass. The insulator layer was 300 nm thick, made of plasma-enhanced chemical vapor deposition silicon dioxide (PECVD-SiO_2). ITO (100 nm) and MoW (100 nm) were chosen as S/D electrodes for our devices. The defined channel length and width of both two devices (S/D = ITO, MoW) were 30 and 500 μm. For complete transistors, the organic material was put into the crucible and thermally deposited through a shadow mask in a high vacuum chamber. We maintained the substrate temperature at

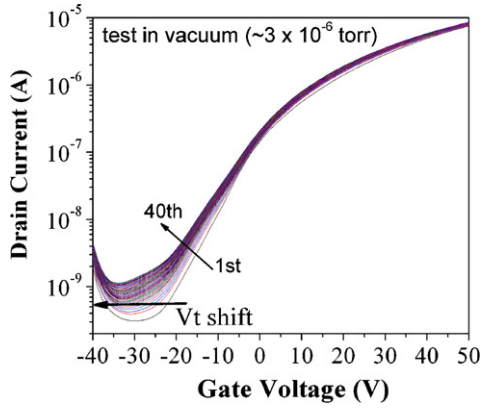

Fig. 4. Transfer characteristics of device reliability which were tested in vacuum environment (3×10^{-6} Torr). Output drain voltage (V_d) was +50 V, and gate voltage swept from −40 to +50 V for each test.

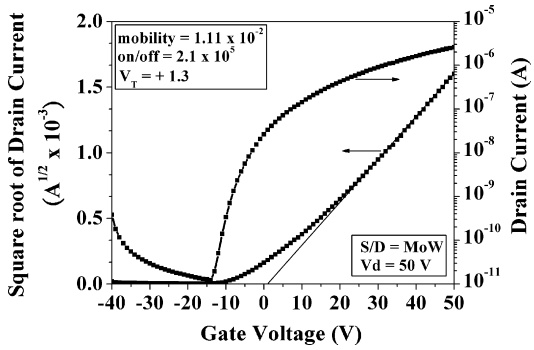

Fig. 5. Transfer characteristics of MoW-based transistors. Inset shows mobility, on/off current ratio (on/off), threshold voltage (V_T), source/drain electrodes (S/D) and drain voltage (V_d).

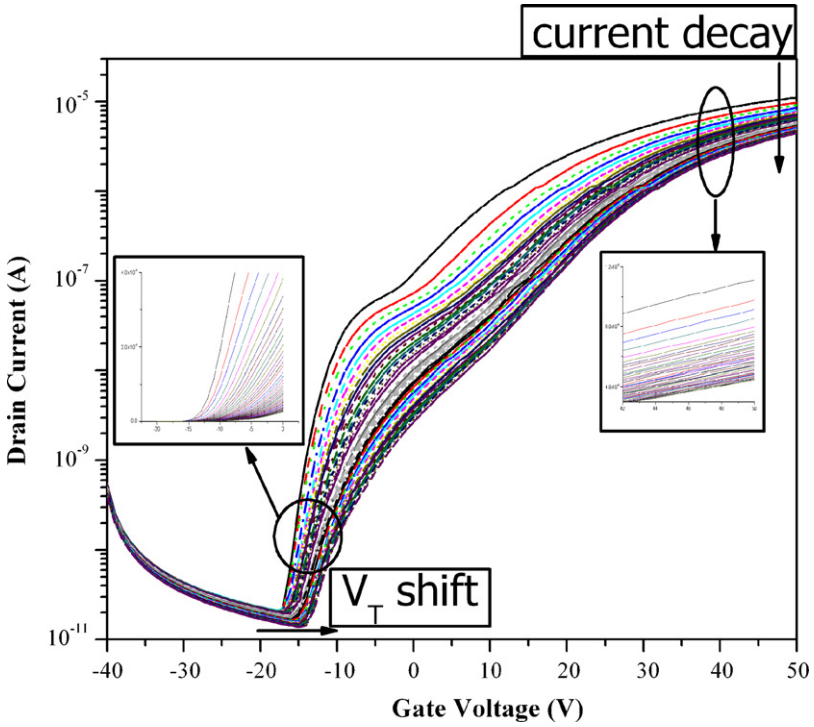

Fig. 3. Transfer characteristics of device reliability, inset shows the shift of turn-on voltage and decay of on-current. Output drain voltage (V_d) was +50 V, and gate voltage swept from −40 to +50 V for each test.

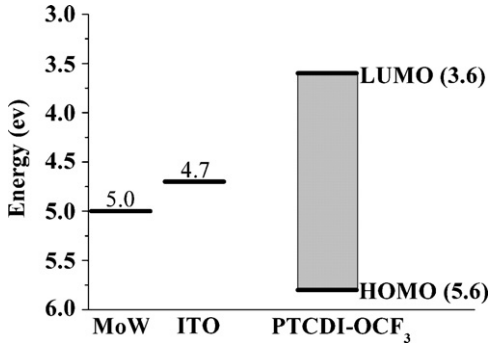

Fig. 6. Energy levels of MoW, ITO and PTCDI-OCF_3.

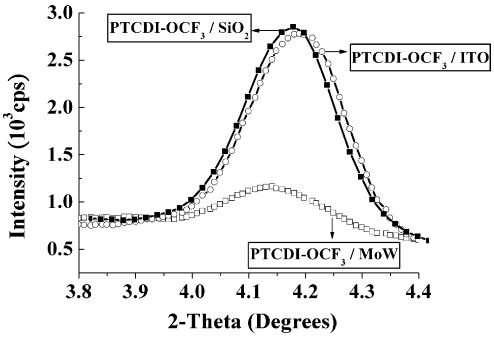

Fig. 7. X-ray diffraction patterns of PTCDI-OCF_3 films growing on selected substrates: SiO_2, ITO and MoW.

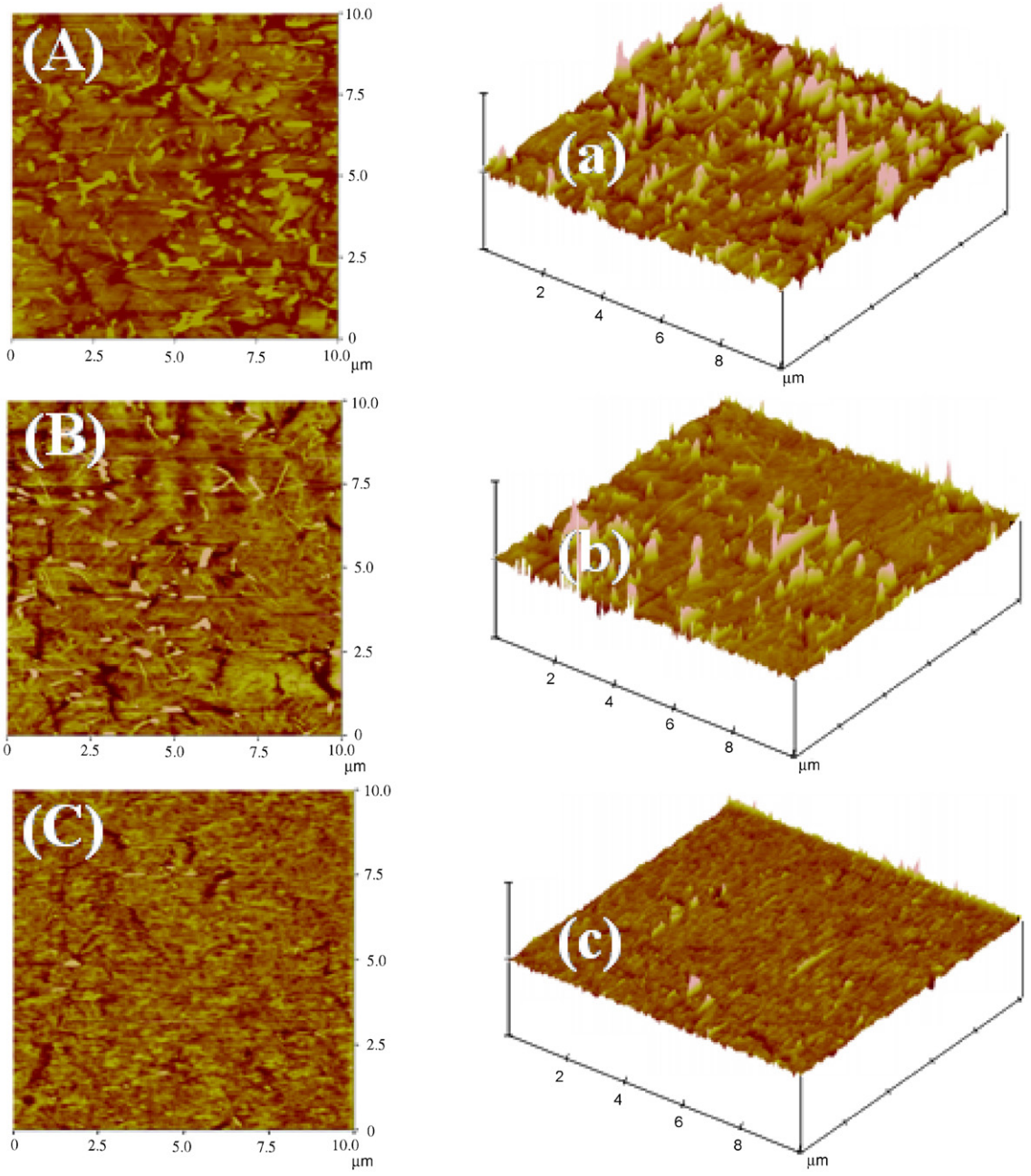

Fig. 8. AFM images (10 μm × 10 μm) of PTCDI-OCF_3 deposited on SiO_2 (A, a), ITO (B, b) and MoW (C, c).

110 °C while PTCDI-OCF_3 evaporated. PTCDI-OCF_3 was prepared following a modified published procedure [12]. Materials were purified via gradient-temperature sublimation which we used as the semiconductor layer.

3. Results and discussion

Most organic n-type devices are fabricated in a top-contact form, in which the source and drain electrodes are defined on top of the semiconductor layer through a shadow mask. In our previous studies, the chemical structure including "–OCF_3" was suitable for bottom-contact devices. Here, the source and drain electrodes were deposited beforehand on the dielectric layer, and then the organic layer was allowed to evaporate fully. On this basis, we synthesized a larger center-core of conjugated system in which a perylene-core was selected in place of the naphthalene-core. The performance of the bottom-contact device with ITO as S/D electrodes showed a high mobility of 3.37×10^{-2} cm^2 V^{-1} s^{-1}, an on/off current ratio of 6.5×10^5, and a threshold voltage of −4.0 V. Improvements of electric characteristics indicated that enlarged conjugated size allowed increased electron flow and that the lowest unoccupied molecular orbital (LUMO) was favorable for n-type organic transistors. Fig. 2 shows the transfer curves of PTCDI-OCF_3, and OTFTs used ITO as S/D electrodes without any further surface treatments of both SiO_2 (SAM) and S/D electrodes (plasma-treatments). We tested reliability of PTCDI-based bottom-contact devices with a continuing bias. Fig. 3 displays the transfer curves of the device when operating totally 40 times. Output drain voltage (V_d) was +50 V, and gate voltage swept from −40 to +50 V for each test. A threshold voltage shift can be seen in each transfer curve, shifting from the left to right side. We also test the OTFT device in vacuum environment (3×10^{-6} Torr). As shows in Fig. 4, output drain voltage and gate voltage were the same as tested in ambient environment. Gate bias stress caused a shift from the right to left side. The results can be seen in previous study, Chestergield et al. have been demonstrated that the common TFT instability of threshold voltage shift was observed for PTCDI-C_5 OTFTs. The deep accept-like trap states in the organic semiconductors may result in a threshold voltage shift [13]. The drop in device on-current appeared to show that the decay of the electric characteristics was mainly damaged by moisture and oxygen from the environment.

In order to further understand electric characteristics of bottom-contact devices, we tried another inorganic metal alloy, MoW as S/D electrodes. OTFTs were fabricated without surface treatments and showed a mobility of 1.11×10^{-2} cm^2 V^{-1} s^{-1}, an on/off current ratio of 2.1×10^5, and threshold voltage of +1.3 V (see Fig. 5). Compared with the ITO-based device, the MoW-based one displayed lower ability in operating. In electron-transporting materials, lowering the work-function of metals to improve the device performance is the usual strategies for organic devices [14]. A higher work function was estimated in metal alloy MoW than in metal ITO. Fig. 6 shows relative energy levels of metal MoW, metal ITO and the organic semiconductor (PTCDI-OCF_3). For electron-transporting OTFTs, S/D electrodes with low work function, were chosen to reduce the barrier between metal/organic contacts. The threshold voltage of the ITO-based device is −4 V which is less than a MoW-based one (+1.3 V). The reduced threshold voltage revealed that the carrier can more easily pass through the metal/semiconductor interface [7,15]. For the same reason, the ITO-based device also shows higher on-current and carrier mobility. Furthermore, to obtain energy levels, the metal work function and the highest occupied molecular orbital (HOMO) of PTCDI-OCF_3 were measured in open air by photoelectron spectroscopy with an ultraviolet source (RKI, model AC-2). The LUMO energy level of PTCDI-OCF_3 was calculated by subtracting the energy band gap of the organic semiconductor.

Fig. 7 shows peaks of X-ray diffraction collected from organic solid-films on the substrate of SiO_2, ITO and MoW, respectively. The intensity of the first diffraction peak growing on SiO_2 and metal ITO was much stronger than that grown on metal MoW. Fig. 8 shows surface morphology of PTCDI-OCF_3 deposited on the SiO_2, ITO, and MoW. Semiconductors grow on the SiO_2, ITO, and MoW, were showed surface roughness of 12.8, 9.46 and 4.06 nm, respectively, estimated through atomic force microscopy (AFM, Digital Instruments Nanoscope). When PTCDI-OCF_3 was deposited on the surface of SiO_2 and ITO, larger grain growth could be found in AFM images (Fig. 8(A, a) and (B, b)). Fig. 8(C, c), however, shows the flat film packing which conforms the low X-ray diffraction. In our experiments, although the varied morphology which appeared in different metal substrate, metal work function seems to employ the major component to the electric characteristic of OTFTs.

4. Conclusions

In summary, we have demonstrated bottom-contact OTFTs with an air-stable organic semiconductor, N,N-bis(4-trifluoromethoxybenzyl)-perylene-3,4,9,10-tetracarboxylic di-imide. High mobility of the ITO-based transistor and the MoW-based transistor were, respectively, 3.37×10^{-2} and 1.11×10^{-2} cm^2 V^{-1} s^{-1}. The on/off current ratio of two OTFTs was more than 10^5. We found that different work functions of S/D electrodes directly influence electric characteristics in device performance. For electron-transporting materials, the metal electrode that has low work function can be chosen as source/drain electrodes in OTFTs.

Acknowledgment

This work was supported by the Display Technology Center for the Industrial Technology Research Institute for Taiwan, ROC (Contract No. 6301XS1F21).

References

[1] H. Kawaguchi, T. Someya, T. Sekitani, T. Sakurai, IEEE J. Solid-State Circuits 40 (2005) 177.
[2] H. Sirringhaus, T. Kawase, R.H. Friend, T. Shimoda, M. Inbasekaran, W. Wu, E.P. Woo, Science 290 (2000) 2123.
[3] G. Horowitz, X.Z. Peng, D. Fichou, F. Garnier, Synth. Met. 51 (1992) 419.
[4] T.W. Kelley, L.D. Boardman, T.D. Dunbar, D.V. Muyres, M.J. Pellerite, T.Y.P. Smith, J. Phys. Chem. B 107 (2003) 5877.
[5] B.K. Crone, A. Dodabalapur, R. Sarpeshkar, R.W. Filas, Y.Y. Lin, Z. Bao, J.H. O'Neill, W. Li, H.E. Katz, J. Appl. Phys. 89 (2001) 5125.
[6] H.E. Katz, A.J. Lovinger, J. Johnson, C. Kloc, T. Siegrist, W. Li, Y.Y. Lin, A. Dodabalapur, Nature 404 (2000) 478.
[7] P.R.L. Malenfant, C.D. Dimitrakopoulos, J.D. Gelorme, L.L. Kosbar, T.O. Graham, A. Curioni, W. Andreoni, Appl. Phys. Lett. 80 (2002) 2517.
[8] S.B. Heidenhain, Y. Sakamoto, T. Suzuki, A. Miura, H. Fujikawa, T. Mori, S. Tokito, Y. Taga, J. Am. Chem. Soc. 122 (2000) 10240.
[9] B. Yoo, T. Jung, D. Basu, A. Dodabalapur, B.A. Jones, A. Facchetti, M.R. Wasielewski, T.J. Marks, Appl. Phys. Lett. 88 (2006) 082104.
[10] C.C. Kao, P. Lin, C.C. Lee, Y.K. Wang, J.C. Ho, Y.Y. Shen, Appl. Phys. Lett. 90 (2007) 212101.
[11] B.A. Jones, M.J. Ahrens, M.-H. Yoon, A. Facchetti, T.J. Marks, M.R. Wasielewski, Angew. Chem. Int. Ed. 43 (2004) 6363.
[12] J. van Herrikhuyzen, A. Syamakumari, A.P.H.J. Schenning, E.W. Meijer, J. Am. Chem. Soc. 126 (2004) 10021.
[13] R.J. Chesterfield, J.C. Mckeen, C.R. Newman, C.D. Frisbie, P.C. Ewbank, K.R. Mann, L.L. Miller, J. Appl. Phys. 95 (2004) 6396.
[14] C. Rost, D.J. Gundlach, S. Karg, W. Rieβ, J. Appl. Phys. 95 (2004) 5782.
[15] L. Torsi, A. Dodabalapur, H.E. Katz, J. Appl. Phys. 78 (1995) 1088.

Chia-Chun Kao[a]
Pang Lin[a]
Yu-Yuan Shen[b]
Jing-Yi Yan[b]
Jia-Chong Ho[b]
Cheng-Chung Lee[b,*]
Li-Hsin Chan[c]
[a] *Department of Materials Science and Engineering, National Chiao-Tung University, Hsinchu, Taiwan*
[b] *Process Technology Division, Display Technology Center, Industrial Technology Research Institute, Hisinchu, Taiwan*
[c] *Department of Applied Materials and Electro-Optical Engineering, National Chi-Nan University, Nantou, Taiwan*

[*] Corresponding author. Fax: +886 3 5826842.
E-mail address: leecc@itri.org.tw (C.-C. Lee)

4 December 2007

16 July 2008

25 August 2008

Available online 23 October 2008